IEEE Access
Multidisciplinary : Rapid Review : Open Access Journal

Received 18 June 2022, accepted 5 July 2022, date of publication 12 July 2022, date of current version 21 July 2022.

Digital Object Identifier 10.1109/ACCESS.2022.3190082

RESEARCH ARTICLE

Torque Ripple Suppression of Switched Reluctance Motor Based on Fuzzy Indirect Instant Torque Control

BENQIN JING[1,2], XUANJU DANG[1], ZHENG LIU[2], AND SHIKE LONG[1,2]

[1]School of Electronic Engineering and Automation, Guilin University of Electronic Technology, Guilin 541004, China
[2]School of Electronic Information and Automation, Guilin University of Aerospace Technology, Guilin 541004, China

Corresponding author: Xuanju Dang (xjd69@163.com)

This work was supported in part by the National Natural Science Foundation of China under Grant 61863008 and Grant 61863007, in part by the Guangxi Natural Science Foundation under Grant 2020GXNSFAA297032, and in part by the Fundamental Ability Enhancement Project for Young and Middle-Aged University Teachers in Guangxi Province under Grant 2021KY0801 and Grant 2021KY0793.

ABSTRACT High torque ripple limits the industrial application of switched reluctance motor (SRM) due to the deep magnetic saturation. This paper proposes a fuzzy indirect instant torque control (IITC) to suppress torque ripple. First, a fuzzy controller is developed to generate a compensation current according to the torque error. The input factor is then proposed and combined with artificial experience. Moreover, considering the relationship between current and electromagnetic torque, the output factor is appropriately designed according to the linearized inductance derivative. Finally, based on a three-phase 12/8 SRM, simulation and experimental results are provided to demonstrate the effectiveness of the proposed fuzzy IITC at torque ripple suppression. Compared with traditional proportion differentiation (PD) IITC, the fuzzy IITC proves its superiority in reducing torque ripple.

INDEX TERMS Fuzzy compensation, indirect instant torque control, switched reluctance motor, current sharing function.

I. INTRODUCTION

Switched reluctance motor (SRM) has the characteristics of solid durability, simple structure, and no need for rare metal manufacturing [1], [2], which is environmentally friendly. Therefore, it has received significant attention and is expected to become a potential choice for the next generation of electric vehicles [3], [4]. However, severe torque ripple limits its performance and application range. To solve this problem, many methods are designed, including torque sharing function (TSF), current profile method, indirect instant torque control (IITC), and various other control methods [5], [6].

The TSF method assigns the torque to each phase according to the mathematical function selective and the distribution function target to provide constant total torque. The distribution function significantly influences the torque ripple [7]. According to the trade-off between copper loss and torque-speed performance in TSF, the Tikhonov coefficient is selected to reduce copper loss and torque ripple [8]. Furthermore, the genetic algorithm can be employed to optimize the conduction and overlap angle to minimize the effective change rate of the magnetic chain and the square of the root mean square current. The influence of adjusting the weight factor of the fitness function on copper loss and torque ripple under different torque distribution functions is also compared in [9]. However, the above two methods are highly dependent on motor parameters, so they need to be re iterated when transplanted to other motors. To solve this problem, the torque error is introduced into the control system. The Hermite interpolation method estimated the instantaneous phase torque of rotor position and obtained the reference phase torque by TSF [10]. Distributing the current by the motor's static flux linkage characteristics obtained from the finite element analysis and experiment describing the motor dynamics can suppress the torque ripple and minimizes copper loss [11].

The associate editor coordinating the review of this manuscript and approving it for publication was Haibin Sun.

This work is licensed under a Creative Commons Attribution 4.0 License. For more information, see https://creativecommons.org/licenses/by/4.0/

Unlike the TSF method, the current profile method is another effective indirect torque method to determine the reference current directly. Usually, the current profile method starts with a simple reference current and requires fine-tuning to achieve the final reference current with good torque control performance. Based on the current reference, the constraint condition is set to minimize the torque ripple, and then through a genetic algorithm, the optimal current shape can be obtained [12]. The high-speed performance is improved by considering the current change rate [13]. By deducing the reference current and optimizing the rotor shape, the method can reduce the torque ripple, inhibit the bus current ripple, and minimize the copper loss [14]. However, this method is only suitable for SRM under an unsaturated state. By representing the phase current as a group of small Fourier coefficients instead of a set of significant discrete points, better steady-state convergence of current waveform and lower torque ripple can be realized [15]. To improve SRM in high-speed operation and effectively reduce torque ripple, a neural network with cerebellar model articulation is used to learn the rate function on the rotor angle of the controlled motor [16]. Model predictive control (MPC) algorithm can also be proposed to minimize torque ripple with its optimal duty cycle based on pulse width modulation (PWM) for delta modulation [17]. Moreover, by selecting the best candidate voltage vectors, MPC can avoid the complex switching rules and reduce torque ripple [18]. In [19], according to the current distribution required in SRM operation, the contour is fine-tuned in the coupling simulation of finite element and dynamic controller. This method considers nonlinearity, electrical loss, magnetic loss, and mutual coupling fully. Current and flux linkage common control methods control the SRM without model information [20]. However, using the flux linkage sharing method (FSM), only the inner loop of the flux linkage can obtain higher control performance. This method realizes the current and flux linkage sharing between the phases of the switched reluctance motor and can reduce the torque ripple to a deficient level. The current profile method is generally developed around the current and phase current characteristics required by SRM. According to the literature cited above, torque ripple can be effectively reduced through compensation or injection, leading to the development of IITC.

With the development of control theory, some nonlinear control methods have been applied to switched reluctance motors to improve the control performance [21], [22]. Fuzzy control has certain robustness to time-varying load and is suitable for controlling nonlinear, time-varying, lagging, and incomplete model systems [23], [24]. Setting fuzzy control based on artificial experience has gradually developed into a mature theory and is widely used in motor control [25]. Fuzzy parameters can initial randomly, and then they can self-adjust to make the controller produce smooth torque and achieve the essential speed of the motor [26]. However, the initial torque error was significant, and the parameter adjustment process persisted long. Furthermore, a novel offline current modulation method for switched reluctance motor based on fuzzy neural compensation is proposed without torque signal [27]. The compensation signal is learned before the regular operation in the self-debugging operation, and the necessary current shape is captured to reduce the torque ripple. However, this method requires plenty of data for offline training. By adding a compensation element to correct the front of the winding current instruction, the goals of reducing the speed ripple level and torque ripple can both be realized [28]. By dividing the conduction interval of each phase into several segments and injecting the harmonic current into the reference current of each phase, an adaptive fuzzy control method for SRM with piece-wise harmonic current injection is proposed in [29]. Considering the difficulty in establishing a complete SRM mathematical model, a modeling method for switched reluctance motor based on an adaptive neural-fuzzy inference system (ANFIS) is proposed [30]. However, this method requires plenty of offline data. Considering that the turn-off angle has a complex relationship with motor speed and current, the turn-off angle compensator method based on fuzzy logic is designed [31], reducing torque ripple by automatically changing the compensation value. TSF combined with fuzzy logic control, the robustness to torque error of the system is improved [32]. However, this method did not fully integrate the relationship between torque and current of SRM, and the effect of output gain has not been thoroughly studied. This paper proposes a fuzzy indirect instant torque control method with simple fuzzy rules based on the above observation. The proposed method can suppress torque ripple effectively by adjusting the total reference current based on torque error.

The main contributions of this paper are

(1) The control structure of total current generated by fuzzy torque compensation and redistribution is constructed. The transformation from reference torque to current is designed as a linear part and nonlinear compensation added to obtain the total current. The linear part is the torque feed-forward control, designed according to the mechanical torque equation. The nonlinear part is the proposed fuzzy compensation, which is compensated based on the torque error and artificial experience.

(2) A fuzzy torque compensator with torque deviation and torque deviation rate as input is designed. Compared with the traditional PD control method, it has a better adaptive ability.

(3) The input factor is based on the torque ripple in traditional TSF and artificial experience. Given the current and reference torque relationship, the output factor is set as double the linearized inductance derivative.

This paper is organized as follows. The limitation of TSF and the principle of IITC is analyzed in Section 2. Then, we give the detail of the proposed fuzzy indirect instant torque control method in Section 3, with simulate result and analysis in Section 4. Experimental result and some suggested improvements are followed in Section 5. Finally we make the conclusion in Section 6.

II. INDIRECT INSTANT TORQUE CONTROL

A. THE LIMITATION OF TSF

TSF is one of the widely used torque ripple suppression methods. TSF distributes the reference torque symmetrically into each phase. Therefore, it is crucial to establish accurate equations of torque and current and rotor position. The reference torque is given by the sum of the individual phase torques.

$$T_e = \sum_{k=1}^{m} T_k(i, \theta) \tag{1}$$

where T_e is the electromagnetic torque, m is the phase number of the SRM, T_e is the electromagnetic torque of phase k, i is the phase current, θ is the rotor position.

Ignoring the saturation of flux linkage and linearizing the inductance partial derivative, the relationship between electromagnetic torque and phase current follows the formula.

$$T = \frac{1}{2} i^2 \frac{\partial L}{\partial \theta} \tag{2}$$

where L is phase inductance.

The given phase current, calculated using the reference torque in formula(2), is then fed into the current hysteresis controller to control the output torque indirectly by controlling the current and suppressing the torque ripple. However, due to the nonlinear inductance, the relationship between the torque and the current and the rotor position is nonlinear. Therefore, due to the inaccuracy of the inductance derivative, the calculated current cannot make the torque reach constant, and the torque ripple is generated.

B. TRADITIONAL PD IITC

For obtaining a constant electromagnetic torque, it is necessary to bring the torque error into a closed-loop control system. In the IITC system, torque error is treated as compensation, as illustrated in Fig. 1.

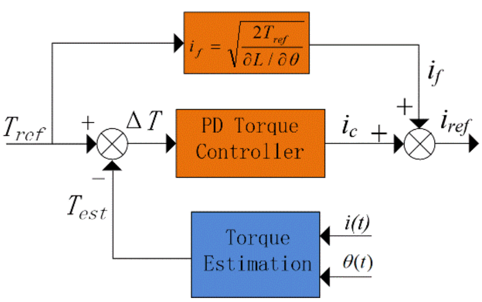

FIGURE 1. Conventional PD IITC method.

There are two routes to calculate the total current, linear transformation, and torque error compensation. First, the inductance partial derivative can be regarded as a constant value in the direct conversion control. Then the current becomes a continual coefficient linear quadratic term of a given torque. The linearization of the inductance partial derivative will inevitably bring in the conversion error. Compensation control is used to adjust the output current according to the torque deviation as a nonlinear compensation current to compensate for the error caused by the inaccurate modeling of inductance deviation. The torque deviation is the difference between the given reference torque and the actual feedback torque, and the actual feedback torque is obtained by looking up the table. There is a nonlinear relationship between torque and current and rotor angle, as shown in Fig. 2. The table can be obtained by measuring the output torque under different rotor position and currents.

The linear transformation part only realizes the linear transformation from the reference torque to the reference current, and the torque error compensation can be corrected by introducing the torque deviation. The formula used for linear transformation is

$$i_f = \sqrt{\frac{2T_{ref}}{\partial L / \partial \theta}} \tag{3}$$

where T_{ref} is the reference torque, $\partial L / \partial \theta$ is the inductance derivatives, i_f is the linear output current.

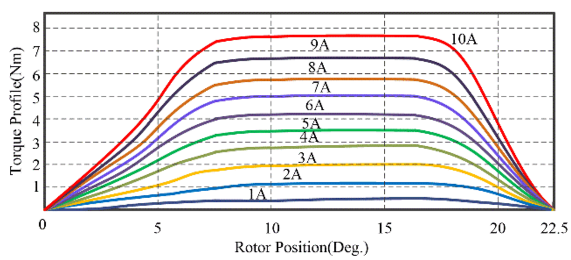

FIGURE 2. Relationship curve of current, rotor position and torque.

The proportion differentiation (PD) controller can convert torque deviation to compensation current. PD controller is a typical model-free controller, and only two parameters need to be adjusted. The output variables of the PD controller can be superposed with the output of the linear controller as compensation, and the sum of superposition is used as the total reference current of SRM. Since there is a nonlinear relationship between the torque deviation and the compensation current, the calculation method based on the model will be complex. Using the model-free control method will reduce calculation and improve the tracking speed of the nonlinear compensation part. The proportional part of PD is to enlarge the error multiple, therefore, the controller can compensate for the error more quickly. The differential part acts according to the trend of error change. The integral function is usually used to eliminate the static error, and the error is accumulated under the condition of constant value. In this system, the nonlinear error compensation part is dynamic, and this part is not static, so the integral part in PID cannot be used.

Once the total current is obtained, phase current can be distributed according to the rotor position. The whole system is shown in Fig. 3.

Unlike the TSF distributing reference torque, current sharing method (CSM) distributes the total current. The total current can be adjusted according to the actual torque of the feedback, which means CSM enables torque compensation.

According to the control system designed by the current distribution method, as shown in Fig. 3. The outer loop is the speed control, and the inner loop is the current control. The output of the speed controller is reference torque, which is used to calculate the total current. There are two steps in the current control loop. First, the current distribution unit is followed by the current calculation. Second, the current is distributed according to the rotor angle and then compared with the feedback current of each phase to form a hysteresis controller.

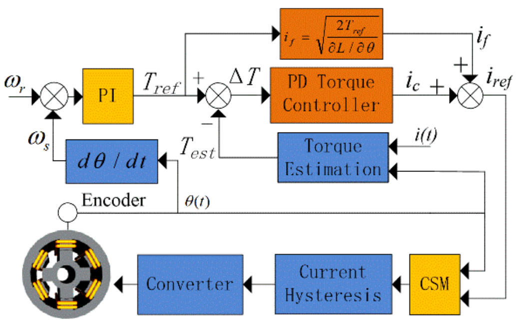

FIGURE 3. Conventional IITC based on PD torque controller.

Similar to TSF, CSM is carried out according to the rotor position.

$$\begin{cases} i_k(\theta) = i_{all} f_k(\theta) & \text{k} = 1, 2, 3, \ldots, \text{m} \\ \sum_{k=1}^{m} f_k(\theta) = 1 & 0 \le f_k(\theta) \le 1 \end{cases} \tag{4}$$

where i_{all} is the reference total current, i_k is the k-phase output current, and f_k is the function of current sharing method.

Referring to the cubic distribution scheme in the TSF, the CSM is designed in which the turn-on angle, turn-off angle, and transition angle are parameters designed manually.

$$f_k(\theta) = \begin{cases} 0 & 0 \le \theta < \theta_{on} \\ 3(\frac{\theta-\theta_{on}}{\theta_{ov}})^2 & \\ -2(\frac{\theta-\theta_{on}}{\theta_{ov}})^3 & \theta_{on} \le \theta < \theta_{on}+\theta_{ov} \\ 1 & \theta_{on}+\theta_{ov} \le \theta < \theta_{off} \\ 1-3(\frac{\theta-\theta_{on}}{\theta_{ov}})^2 & \\ +2(\frac{\theta-\theta_{on}}{\theta_{ov}})^3 & \theta_{off} \le \theta < \theta_{off}+\theta_{ov} \\ 0 & \theta_{off}+\theta_{ov} \le \theta \le \tau_t \end{cases} \tag{5}$$

where θ_{on}, θ_{off} and θ_{ov} are the turn-on angle, turn-off angle and transition angle, respectively.

With the proper CSM, the torque deviation as the input, and the output as the compensation current, the PD controller can reduce the torque ripple to a certain degree. However, the compensated current of each step time from the PD controller is fixed and lagged, resulting in the disability at the rapid response to the torque deviations.

III. FUZZY IITC

A. FUZZY COMPENSATION SYSTEM

The fuzzy controller can be regarded as an evolutionary PD controller, and its input deviation and deviation change rate can be viewed as proportional and differential variables, respectively. Both the proportional and differential can be adjusted according to the deviation and deviation change rate under different torque errors. Compared with the PD controller, the fuzzy controller also introduces the artificial experience value in the design of fuzzy rules, which can be adjusted according to the current value and the expected value, with a predictive control effect. The introduction of this value will make the output result more in line with the expected effect.

The fuzzy control method is used as current compensation, and the input of the fuzzy structure is the torque error and the change rate of the error. The nonlinear feed-forward compensation and control system of the SRM inductance model based on fuzzy rules is shown in Fig. 4.

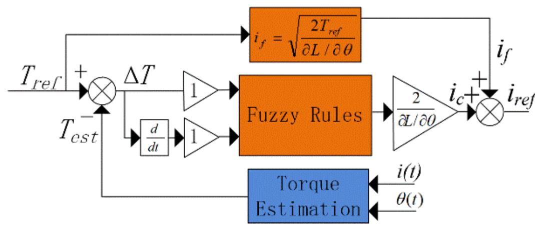

FIGURE 4. Proposed fuzzy indirect instant torque controller.

As the SRM system is current-controlled, the reference total current is no longer a fixed value. It is adjusted in real-time according to the deviation of the current feedback load torque and the given reference torque. As a result, the total current has the characteristics that it is generated according to the needs, which better adapts to the non-linearity of SRM.

B. FUZZY CONTROLLER

As mentioned above, the fuzzy controller is adopted as current compensation in the control loop. The proposed fuzzy controller has fuzzification, fuzzy reasoning, and defuzzification processes. The torque error between torque reference and the accurate torque, together with the torque error change, constitute two fuzzy control inputs. Both the error and the error change rate are normalized by multiplying with the corresponding scaling factors.

Both of the scaling factors of input need to cover the range of torque error adequately. If the scaling factors are too small, the compensation response cannot be well carried out according to the torque error, and the compensation effect will be poor. Conversely, if the scaling factors are too large, the resolution of current compensation is insensitive, and the compensation effect will also be poor.

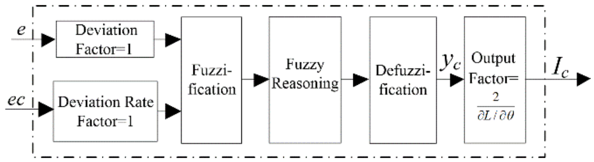

FIGURE 5. Control principle of the fuzzy method.

In the TSF method, the maximum torque ripple can usually reach 100%. Therefore, the torque fluctuation range obtained by subtracting the maximum output from the minimum output torque is equal to the average output torque. Assuming that the average output torque equals the load torque, the input universe can be set as $[-0.5\ 0.5]$. However, due to the motor friction in the natural system, the output torque will be larger than the torque load. Therefore, the average value of the actual electromagnetic torque is usually more significant than the load torque. Therefore, the scaling factors of input need to be expanded to include the torque error range. Considering that the friction is usually a variable value, it is reasonable to set the input universe to $[-1\ 1]$, combined with practical experience. Therefore, both of the scaling factors of input are set to one.

The output scaling factor is designed based on the characteristic of the SRM. Due to the differential action of the fuzzy controller, the compensation current is no longer the square relationship of the torque error but the relationship of fuzzy multiplied by the proportional coefficient. Therefore, combining equations (2) and (3), the relationship between torque error and compensation current can be expressed as (6).

$$I_c = f_2(\frac{2 * \Delta T}{\partial L/\partial\theta}) = \frac{2}{\partial L/\partial\theta} * f_2(\Delta T) \tag{6}$$

Therefore, the total reference current output is

$$I_{all} = I_f + I_c = f_1(\frac{2 * T_{ref}}{\partial L/\partial\theta}) + \frac{2}{\partial L/\partial\theta} f_2(\Delta T) \tag{7}$$

where I_f is linear transformation equation from torque to current, I_c is output of the fuzzy controller, I_{all} is the total reference current. Thus, the output domain is setting the same as the inductance deviation $\partial L/\partial\theta$, which is linearized in the system.

The torque deviation, torque deviation change rate, and output of the fuzzy controller are represented by E, EC, and U, respectively, to simplify the description. Due to the need to balance the performance and computing resources consuming, only five triangular membership functions are designed in fuzzification. The domain of deviation E and EC both are $[-1, +1]$, the membership function is negative big (NB), negative small (NS), zero (ZE), positive small (PS), positive big (PB), the rule table is shown in the Table 1.

The membership function of E, EC, and U are all triangular wave functions.

$$R_i = (E_i \times EC_i)^{T_1} \times U_i \tag{8}$$

TABLE 1. Fuzzy rules table.

E	EC: NB	NS	ZE	PS	PB
NB	NB	NB	NB	NB	NS
NS	NB	NB	NS	NS	ZE
ZE	NB	NB	NS	ZE	PS
PS	NS	ZE	PS	PB	PB
PB	PS	PB	PB	PB	PB

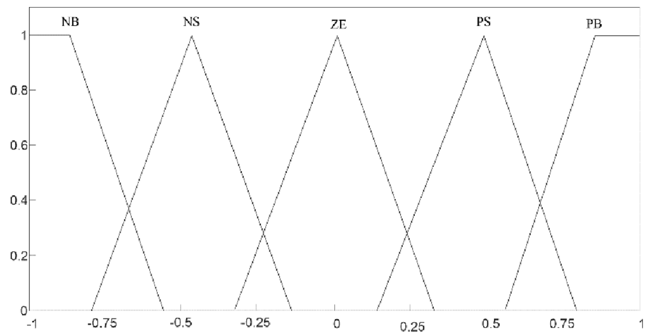

FIGURE 6. Membership function.

By combining all fuzzy rules with the relationship of 'or', the fuzzy relationship R describing the rules of the whole system is

$$R = R_1 \cup R_2 \cup \cdots \cup R_{25} = \bigcup_{i=1}^{25} R_i \tag{9}$$

The output of fuzzy reasoning is

$$U = (E \times EC)^{T_2} \circ R \tag{10}$$

The fuzzy set is obtained by fuzzy reasoning, and the output is determined by the gravity fuzzy judgment method, which is defined as follows

$$y_c = \frac{\sum_{1}^{25} y_i \mu(y_i)}{\sum_{1}^{25} \mu(y_i)} \tag{11}$$

where i is the number of single point sets, y_i is the point of the discrete domain, $\mu(y_i)$ is the membership function value of the corresponding attribute.

The output of the fuzzy compensator is

$$I_c = k_c y_c \tag{12}$$

where k_c is the output factor.

The final reference total current calculation formula is

$$I_{all} = I_f + I_c = \sqrt{T_{ref} * \frac{2}{\partial L/\partial\theta}} + y_c * \frac{2}{\partial L/\partial\theta} \tag{13}$$

Since the output of the fuzzy controller is adjusted according to the torque deviation, the compensation part i_c is in dynamic change, followed by the adjustment of the total reference current.

TABLE 2. Motor parameter.

Notion	Value
Number of phases	3
Number of stator/rotor poles	12/8
Rated voltage	240V
Maximum flux linkage	0.486 V.s
Stator resistance	0.01ohm
Inertia constant	0.0082kg.m.m
Friction constant	0.01N·m.s

IV. SIMULATION RESULTS

To verify the feasibility of the proposed algorithm, a 3-phase 12/8 SRM simulation environment is built in MATLAB/Simulink, as the SRM parameter is shown in Table 2. The rotor position is obtained by measuring the pulse conversion of the encoder. The torque table is established by measuring different currents and rotor position. The parameters of the SRM motor are shown in Table 2. The Inductance deviation $\partial L/\partial\theta$ is linearized and set as 0.1. The proportional parameter P and the integral parameter I in the PI speed controller are 0.31 and 0.74, respectively. The current hysteresis width is 0.1 A. θ_{on}, θ_{off} and θ_{ov} are all selected as 5 degrees.

To ensure a fair comparison with the proposed method, the PD parameters are also optimized and finally chosen as P=0.1, D=0.2.

For describing the torque ripple precisely, a formula is constructed, and the formula to calculate the torque ripple is

$$T_{rip} = \frac{T_{\max} - T_{\min}}{T_{ave}} \times 100\% \tag{14}$$

where T_{rip} is torque ripple, $T_{\max}$ is maximum torque during the measuring circle, $T_{\min}$ is minimum torque during the measuring circle, T_{ave} is average torque during the measuring circle.

Fig. 7 shows the phase current and total torque with the traditional PD IITC and the proposed method at 900 rpm and 1Nm.

In this paper, $T_{\max}$, $T_{\min}$ and T_{ave} are calculated by MATLAB using the simulation results. Figs. 7 plots the curves of phase current and torque ripple under different control schemes, respectively. Torque ripple generating primarily at the commutation stage, as we estimated. By changing the compensated current according to torque error, torque ripple can be suppression effectively. For the proposed fuzzy IITC, the maximum-minimum and average total torque are 2.02 Nm, 1.84 Nm, and 1.94 Nm, respectively. They are 2.05 Nm, 1.72 Nm, and 1.96 Nm, respectively, in the PD IITC. The torque ripple results with the proposed fuzzy IITC and PD IITC being 9.5% and 17%, respectively. It shows that the proposed control schemes yield excellent torque ripple reduction compared to the conventional PD IITC method.

In this article, the instantaneous torque is obtained from the look-up table, which contains the static torque characteristics of the SRM prototype, namely the relationship between the instantaneous torque, phase current, and rotor position.

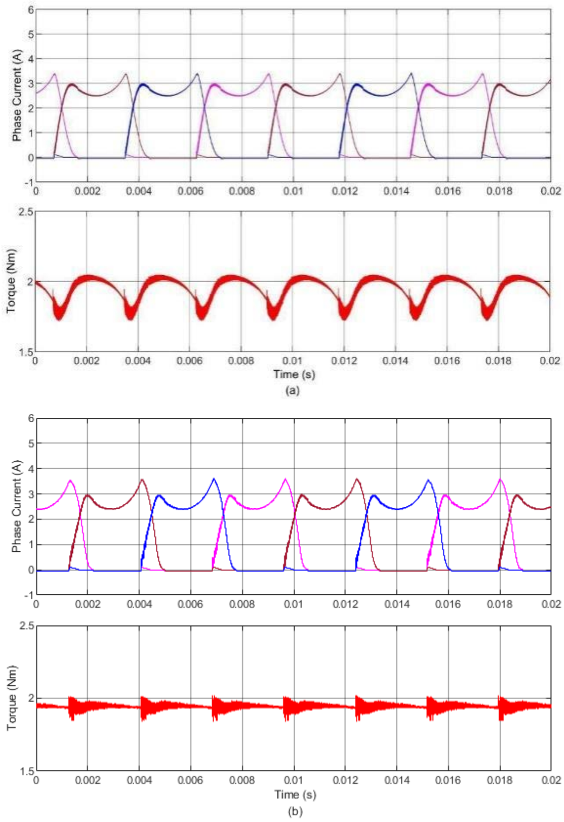

FIGURE 7. Phase current and total torque at 900 rpm and 1Nm with simulation. (a) Traditional PD IITC. (b) Proposed method.

To verify the effectiveness of the proposed method performs well under different conditions, the reference speed is changed to 500 rpm, and the torque load is changed to 3 Nm. Under this condition, the maximum, minimum, and average total torque is 3.58 Nm, 3.4 Nm, and 3.5 Nm, respectively, with the proposed fuzzy IITC. In contrast, they are 3.68 Nm, 3.16 Nm, and 3.52 Nm, respectively, in the PD IITC. Torque ripple with proposed fuzzy IITC and PD IITC is 4.9% and 14.9%, respectively. It shows that the torque ripple decreases as the torque load increases. At the same time, the proposed control schemes yield excellent torque ripple reduction compared with the conventional PD IITC method. The comparison of torque ripple suppression effect is shown in Table 3.

In order to verify the anti-interference performance of the algorithm, the interference current signal is added to the control loop, and the result is shown in Fig. 9. At 0.005s, a 2A step current is added to the feedback of the current hysteresis loop, and the interference signal is ended at 0.01s. Therefore, the current interference value can be regarded as interference or measurement error. Through the results, it can be observed that the output torque of the PD compensation controller is followed by severe shaking. In contrast, the output torque of the fuzzy compensator is rarely affected, maintaining the normal output torque.

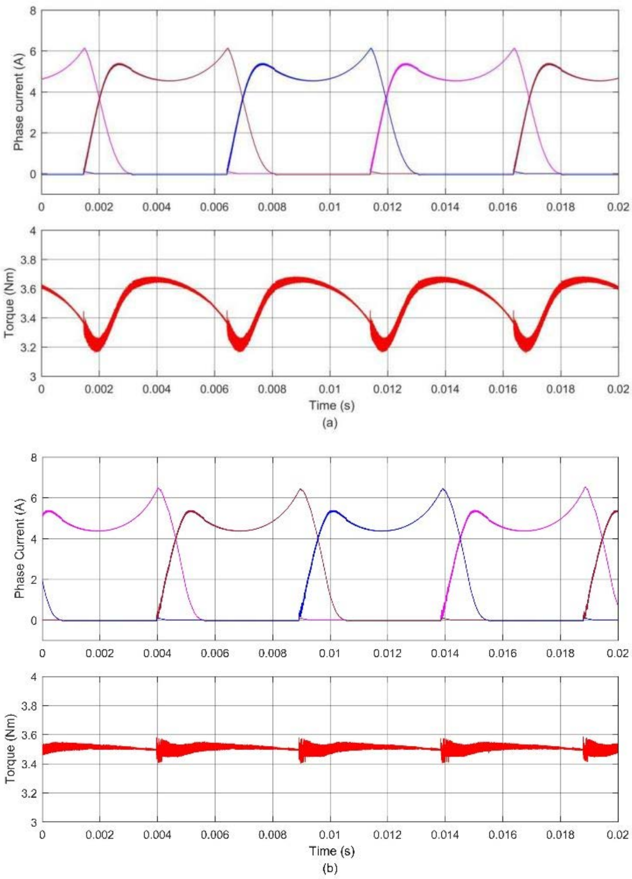

FIGURE 8. Phase current and total torque at 500 rpm and 3Nm with simulation. (a) Traditional PD IITC. (b) Proposed method.

TABLE 3. Torple ripple under different condition.

Method	Trip at 900rpm,1Nm	Trip at 500rpm,3Nm
PD IITC	17%	14.9%
Proposed Method	9.5%	4.9%

With the extension of SRM service time, its internal parameters will also change. To verify the sensitivity of the control algorithm to the change of internal parameters, the output torque under the two algorithms is compared by changing the inertia and friction coefficient of the motor. It is found that changing the inertia does not affect the stability of the output torque, the torque ripple remains unchanged, and changing the friction coefficient will make the electromagnetic torque curve move up and down as a whole, The torque ripple is basically unchanged.

Compared with PD compensation control, fuzzy compensation control can quickly adjust the output according to the deviation and change of input torque so that the compensation value can meet the system requirements and reduce the torque ripple.

V. EXPERIMENT RESULTS

The effectiveness of the PD IITC and proposed fuzzy IITC have been validated by simulation. To further verify the superiority of the proposed fuzzy IITC composite speed control strategy, the comparisons between it and the PD IITC controller are conducted in the experiment.

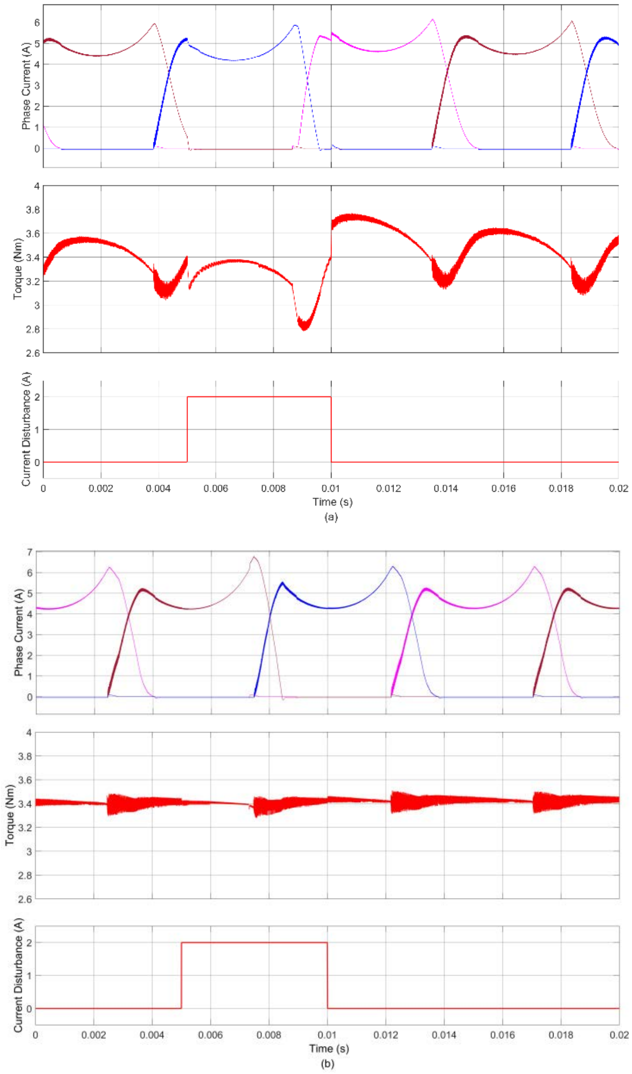

FIGURE 9. Effect of the disturbance on the torque. (a) Traditional PD IITC. (b) Proposed method.

The results mainly include phase current and torque at the stable operation stage. During the experiment, the traditional PD IITC and the proposed fuzzy IITC control strategies are programmed in the STM32F407 control system, respectively. The exact speed and control parameters are applied to both the control strategies to make an impartial and forthright comparison. Figs. 11 and 12 illustrate the experimental results recorded by the oscilloscope.

The performances of the proposed algorithm are applied to a three-phase 12/8 SRM. Fig. 10 shows the test platform, where the HX901 torque-meter with 5 Nm torque range and LEESUN-PB025 magnetic powder brake with 10 Nm torque range is connected by two couplings. The E6B2-CWZ6C encoder detects the position with the STM32 encoder mode.

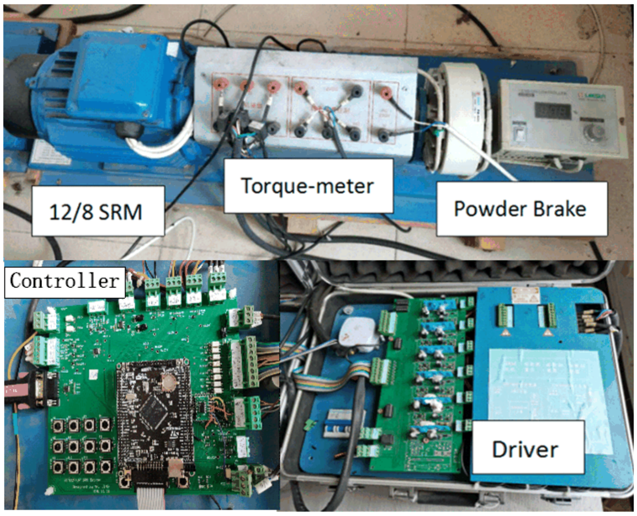

FIGURE 10. Devices and platform for experimental.

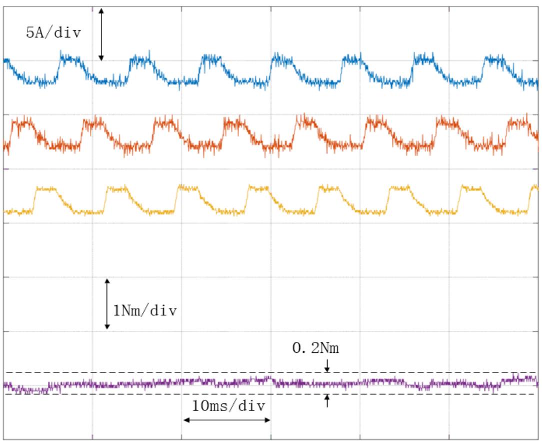

(a)

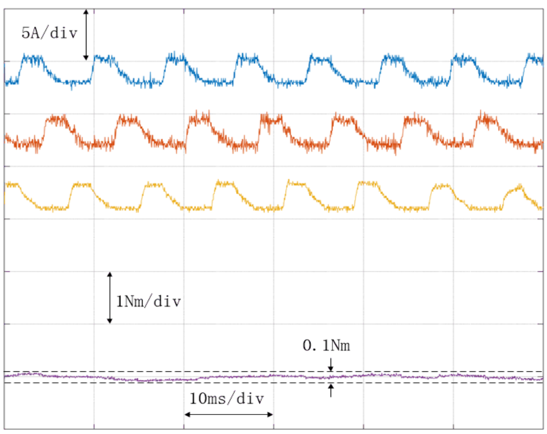

(b)

FIGURE 11. Comparison of experiment results at 900r/min with 1N.m load. (a) PD IITC method. (b) Fuzzy IITC method.

Similarly, the current signal captured by the current sensor is sent to them for further control. The algorithm is implemented in an ARM STM32F407 single-chip microcomputer, with a sampling time setting as 40 us. Other hardware includes a DC power supply, an asymmetrical half-bridge circuit, a PC, and an oscilloscope.

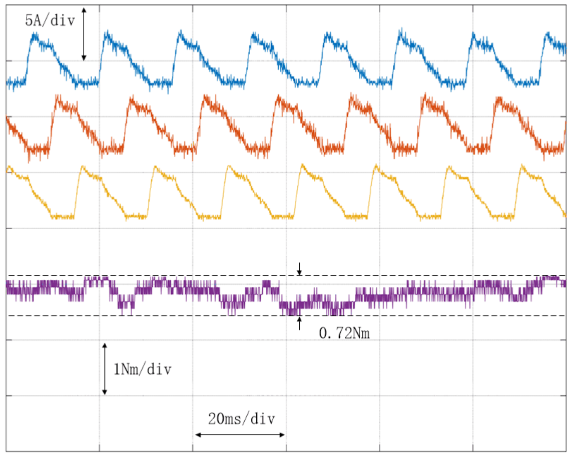

(a)

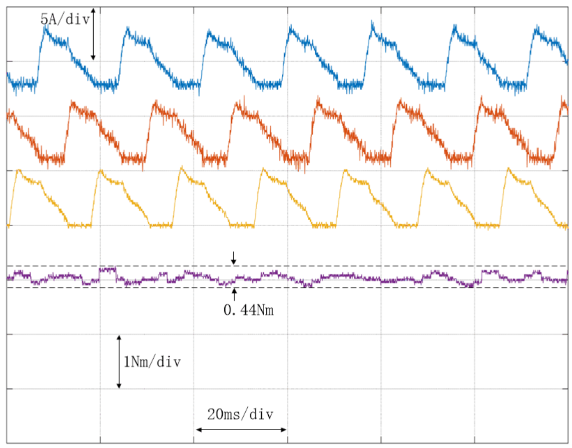

(b)

FIGURE 12. Comparison of experiment results at 500r/min with 3N.m load. (a) PD IITC method. (b) Fuzzy IITC method.

The experimental results for the proposed fuzzy IITC and PD IITC at 900 rpm speed and 1Nm torque load are shown in Fig. 11. The 3-phase currents and electromagnetic torque waveform are shown in Fig. 11(a) and (b), respectively. A significant torque ripple of about 20% can be observed with the PD IITC method. On the other hand, the torque ripple can be suppressed low to about 10% with the proposed fuzzy IITC method. Due to the incorrect parameters and methods is more significant than the simulation. However, the results show that the proposed fuzzy IITC can minimize the torque ripple.

To further verify the effectiveness of the proposed algorithm under different conditions, speed is set to 500rpm and load torque 3N.m.

Fig. 12 illustrates the phase current and torque ripple of the two control schemes in terms of the same rates and load torque. As shown, with the condition changed, the proposed algorithm can maintain a lower torque ripple of about 15%, compared with the torque ripple of about 24% under the PD IITC method. The fuzzy IITC is working satisfactorily as compared to the PD IITC algorithm in maintaining a low torque ripple, which validates the practical effectiveness of the proposed fuzzy IITC.

VI. CONCLUSION

In this paper, a fuzzy IITC method with input factor pre-setting by human experience and output factor pre-setting by inductance deviation was proposed to reduce the torque ripple of the SRM drive system. We can draw the following conclusions through the theoretical analysis and discussions of the simulation and experimental results.

(1) The torque ripple can be effectively reduced by using feed-forward calculation and current compensation. The feed-forward current is calculated based on the electromagnetic torque equation, and the compensation current can be calculated based on the torque error.

(2) The fuzzy control can be used to calculate the compensation current, the fuzzy output factor can be set to twice the linearization value of the inductance derivative, and the input factor can be set to 1 according to the manual experience, which can simplify the design of the fuzzy controller and reduce the amount of calculation.

(3) As demonstrated by the simulation and validated by the experimental test, the proposed fuzzy IITC control strategy performs well in torque ripple reduction since it can effectively compensate for the current.

REFERENCES

[1] E. Bostanci, M. Moallem, A. Parsapour, and B. Fahimi, "Opportunities and challenges of switched reluctance motor drives for electric propulsion: A comparative study," *IEEE Trans. Transport. Electrific.*, vol. 3, no. 1, pp. 58–75, Mar. 2017.

[2] N. Yan, X. Cao, and Z. Deng, "Direct torque control for switched reluctance motor to obtain high torque–ampere ratio," *IEEE Trans. Ind. Electron.*, vol. 66, no. 7, pp. 5144–5152, Jul. 2019.

[3] X. Dang, Y. Shi, and H. Peng, "Torque–flux linkage recurrent neural network adaptive inversion control of torque for switched reluctance motor," *IET Electr. Power Appl.*, vol. 14, no. 9, pp. 1612–1623, Sep. 2020.

[4] J.-W. Ahn and G. F. Lukman, "Switched reluctance motor: Research trends and overview," *CES Trans. Elect. Mach. Syst.*, vol. 2, no. 4, pp. 339–347, Dec. 2018.

[5] G. Fang, F. P. Scalcon, D. Xiao, R. Vieira, H. Grundling, and A. Emadi, "Advanced control of switched reluctance motors (SRMs): A review on current regulation, torque control and vibration suppression," *IEEE Open J. Ind. Electron. Soc.*, vol. 2, pp. 280–301, 2021.

[6] S. Dhale, B. Nahid-Mobarakeh, and A. Emadi, "A review of fixed switching frequency current control techniques for switched reluctance machines," *IEEE Access*, vol. 9, pp. 39375–39391, 2021.

[7] M. Dowlatshahi, S. M. S. Nejad, and J.-W. Ahn, "Torque ripple minimization of switched reluctance motor using modified torque sharing function," in *Proc. 21st Iranian Conf. Electr. Eng. (ICEE)*, Mashhad, Iran, May 2013, pp. 1–6.

[8] J. Ye, B. Bilgin, and A. Emadi, "An offline torque sharing function for torque ripple reduction in switched reluctance motor drives," *IEEE Trans. Energy Convers.*, vol. 30, no. 2, pp. 726–735, Jun. 2015.

[9] X. D. Xue, K. W. E. Cheng, and S. L. Ho, "Optimization and evaluation of torque-sharing functions for torque ripple minimization in switched reluctance motor drives," *IEEE Trans. Power Electron.*, vol. 24, no. 9, pp. 2076–2090, Sep. 2009.

[10] S. Song, R. Hei, R. Ma, and W. Liu, "Model predictive control of switched reluctance starter/generator with torque sharing and compensation," *IEEE Trans. Transport. Electrific.*, vol. 6, no. 4, pp. 1519–1527, Dec. 2020.

[11] H. Li, B. Bilgin, and A. Emadi, "An improved torque sharing function for torque ripple reduction in switched reluctance machines," *IEEE Trans. Power Electron.*, vol. 34, no. 2, pp. 1635–1644, Feb. 2019.

[12] Z. Xia, B. Bilgin, S. Nalakath, and A. Emadi, "A new torque sharing function method for switched reluctance machines with lower current tracking error," *IEEE Trans. Ind. Electron.*, vol. 68, no. 11, pp. 10612–10622, Nov. 2021.

[13] S. Mehta, M. A. Kabir, and I. Husain, "Extended speed current profiling algorithm for low torque ripple SRM using model predictive control," in *Proc. IEEE Energy Convers. Congr. Expo. (ECCE)*, Portland, OR, USA, Sep. 2018, pp. 4558–4563.

[14] T. Kusumi, T. Hara, K. Umetani, and E. Hiraki, "Simultaneous tuning of rotor shape and phase current of switched reluctance motors for eliminating input current and torque ripples with reduced copper loss," *IEEE Trans. Ind. Appl.*, vol. 56, no. 6, pp. 6384–6398, Nov. 2020.

[15] P. L. Chapman and S. D. Sudhoff, "Design and precise realization of optimized current waveforms for an 8/6 switched reluctance drive," *IEEE Trans. Power Electron.*, vol. 17, no. 1, pp. 76–83, Jan. 2002.

[16] C. Shang, D. Reay, and B. Williams, "Adapting CMAC neural networks with constrained LMS algorithm for efficient torque ripple reduction in switched reluctance motors," *IEEE Trans. Control Syst. Technol.*, vol. 7, no. 4, pp. 401–413, Jul. 1999.

[17] X. Li and P. Shamsi, "Model predictive current control of switched reluctance motors with inductance auto-calibration," *IEEE Trans. Ind. Electron.*, vol. 63, no. 6, pp. 3934–3941, Jun. 2016.

[18] A. Xu, C. Shang, J. Chen, J. Zhu, and L. Han, "A new control method based on DTC and MPC to reduce torque ripple in SRM," *IEEE Access*, vol. 7, pp. 68584–68593, 2019.

[19] R. Mikail, I. Husain, Y. Sozer, M. S. Islam, and T. Sebastian, "Torque-ripple minimization of switched reluctance machines through current profiling," *IEEE Trans. Ind. Appl.*, vol. 49, no. 3, pp. 1258–1267, May 2013.

[20] J.-J. Wang, "A common sharing method for current and flux-linkage control of switched reluctance motor," *Electr. Power Syst. Res.*, vol. 131, pp. 19–30, Feb. 2016.

[21] C.-H. Lin, "Adaptive nonlinear backstepping control using mended recurrent romanovski polynomials neural network and mended particle swarm optimization for switched reluctance motor drive system," *Trans. Inst. Meas. Control*, vol. 41, no. 14, pp. 4114–4128, Oct. 2019.

[22] A. K. Rana and A. V. R. Teja, "A mathematical torque ripple minimization technique based on a nonlinear modulating factor for switched reluctance motor drives," *IEEE Trans. Ind. Electron.*, vol. 69, no. 2, pp. 1356–1366, Feb. 2022.

[23] V. K. Jonnalagadda, V. K. Elumalai, H. Singh, and A. Prasad, "Nonlinear control design using Takagi-Sugeno fuzzy applied to under-actuated visual servo system," *Trans. Inst. Meas. Control*, vol. 42, no. 15, pp. 2969–2983, Nov. 2020.

[24] M. Hamdy, S. Abd-Elhaleem, and M. Fkirin, "Time-varying delay compensation for a class of nonlinear control systems over network via H_∞ adaptive fuzzy controller," *IEEE Trans. Syst., Man, Cybern., Syst.*, vol. 47, no. 8, pp. 2114–2124, Aug. 2017.

[25] C.-L. Tseng, S.-Y. Wang, S.-C. Chien, and C.-Y. Chang, "Development of a self-tuning TSK-fuzzy speed control strategy for switched reluctance motor," *IEEE Trans. Power Electron.*, vol. 27, no. 4, pp. 2141–2152, Apr. 2012.

[26] S. Mir, M. E. Elbuluk, and I. Husain, "Torque-ripple minimization in switched reluctance motors using adaptive fuzzy control," *IEEE Trans. Ind. Appl.*, vol. 35, no. 2, pp. 461–468, Mar. 1999.

[27] L. O. A. P. Henriques, P. J. C. Branco, L. G. B. Rolim, and W. I. Suemitsu, "Proposition of an offline learning current modulation for torque-ripple reduction in switched reluctance motors: Design and experimental evaluation," *IEEE Trans. Ind. Electron.*, vol. 49, no. 3, pp. 665–676, Jun. 2002.

[28] J. Chai and C. Liaw, "Reduction of speed ripple and vibration for switched reluctance motor drive via intelligent current profiling," *IET Electr. Power Appl.*, vol. 4, no. 5, pp. 380–396, 2010.

[29] M. Ma, F. Ling, F. Li, and F. Liu, "Torque ripple suppression of switched reluctance motor by segmented harmonic currents injection based on adaptive fuzzy logic control," *IET Electr. Power Appl.*, vol. 14, no. 2, pp. 325–335, Feb. 2020.

[30] W. Ding and D. Liang, "Modeling of a 6/4 switched reluctance motor using adaptive neural fuzzy inference system," *IEEE Trans. Magn.*, vol. 44, no. 7, pp. 1796–1804, Jul. 2008.

[31] M. Rodrigues, P. J. C. Branco, and W. Suemitsu, "Fuzzy logic torque ripple reduction by turn-off angle compensation for switched reluctance motors," *IEEE Trans. Ind. Electron.*, vol. 48, no. 3, pp. 711–715, Jun. 2001.

[32] H.-S. Ro, K.-G. Lee, J.-S. Lee, H.-G. Jeong, and K.-B. Lee, "Torque ripple minimization scheme using torque sharing function based fuzzy logic control for a switched reluctance motor," *J. Electr. Eng. Technol.*, vol. 10, no. 1, pp. 118–127, Jan. 2015.

BENQIN JING received the M.Sc. degree in detection technology and automatic equipment from the University of Electronic Science and Technology of China, Chengdu, China, in 2010. He is currently pursuing the Ph.D. degree in instrument science and technology with the School of Electronic Engineering and Automation, Guilin University of Electronic Technology, Guilin, China.

He is currently a Lecturer with the School of Electronic Information and Automation, Guilin University of Aerospace Technology. He has published more than five papers and holds three patents. His research interests include embedded control technology and intelligent control of switched reluctance motor.

XUANJU DANG received the M.Sc. degree from the Shaanxi University of Science and Technology, Xi'an, China, in 1989, and the Ph.D. degree from Shanghai Jiao Tong University, Shanghai, China, in 2006.

He is currently a Professor with the School of Electronic Engineering and Automation, Guilin University of Electronic Technology. He has published more than 60 papers and holds 36 patents. His research interests include complex systems modeling and control, neural networks modeling and design, and the intelligent control of switched reluctance motor.

ZHENG LIU received the M.Sc. degree from the Guilin University of Technology, Guilin, China, in 2007, and the Ph.D. degree from the Guilin University of Electronic Technology, Guilin, in 2019.

He is currently a Professor with the School of Electronic Engineering and Automation, Guilin University of Aerospace Technology. He has published more than 20 papers and holds two patents. His research interests include nonlinear systems filtering technology and the control theory of power battery energy management systems.

SHIKE LONG received the M.Sc. degree in control science and engineering from the Beijing University of Aeronautics and Astronautics, Beijing, China, in 2016. He is currently pursuing the Ph.D. degree in instrument science and technology with the School of Electronic Engineering and Automation, Guilin University of Electronic Technology, Guilin, China.

He is currently a Lecturer with the School of Electronic Information and Automation, Guilin University of Aerospace Technology. He has published more than five papers and holds two patents. His research interests include systems stability control and intelligent control of manipulator.